Regulation of GPCR expression through an interaction with CCT7, a subunit of the CCT/TRiC complex

Samuel Génier[a], Jade Degrandmaison[a], Pierrick Moreau[a], Pascale Labrecque[a], Terence E. Hébert[b], and Jean-Luc Parent[a,*]

[a]Service de Rhumatologie, Département de Médecine, Faculté de Médecine et des Sciences de la Santé, Université de Sherbrooke, Centre de Recherche du Centre Hospitalier Universitaire de Sherbrooke (CR-CHUS), and Institut de Pharmacologie de Sherbrooke, Sherbrooke, QC J1H 5N4, Canada; [b]Department of Pharmacology and Therapeutics, McGill University, Montréal, QC H3G 1Y6, Canada

ABSTRACT **Mechanisms that prevent aggregation and promote folding of nascent G protein–coupled receptors (GPCRs) remain poorly understood. We identified chaperonin containing TCP-1 subunit eta (CCT7) as an interacting partner of the β-isoform of thromboxane A_2 receptor (TPβ) by yeast two-hybrid screening. CCT7 coimmunoprecipitated with overexpressed TPβ and β_2-adrenergic receptor (β_2AR) in HEK 293 cells, but also with endogenous β_2AR. CCT7 depletion by small interfering RNA reduced total and cell-surface expression of both receptors and caused redistribution of the receptors to juxtanuclear aggresomes, significantly more so for TPβ than β_2AR. Interestingly, Hsp90 coimmunoprecipitated with β_2AR but virtually not with TPβ, indicating that nascent GPCRs can adopt alternative folding pathways. In vitro pull-down assays showed that both receptors can interact directly with CCT7 through their third intracellular loops and C-termini. We demonstrate that Trp^{334} in the TPβ C-terminus is critical for the CCT7 interaction and plays an important role in TPβ maturation and cell-surface expression. Of note, introducing a tryptophan in the corresponding position of the TPα isoform confers the CCT7-binding and maturation properties of TPβ. We show that an interaction with a subunit of the CCT/TCP-1 ring complex (TRiC) chaperonin complex is involved in regulating aggregation of nascent GPCRs and in promoting their proper maturation and expression.**

Monitoring Editor
Adam Linstedt
Carnegie Mellon University

Received: Apr 12, 2016
Revised: Sep 22, 2016
Accepted: Sep 26, 2016

This article was published online ahead of print in MBoC in Press (http://www.molbiolcell.org/cgi/doi/10.1091/mbc.E16-04-0224) on October 5, 2016.

*Address correspondence to: Jean-Luc Parent (jean-luc.parent@usherbrooke.ca).

Abbreviations used: β_2AR, β_2-adrenergic receptor; BSA, bovine serum albumin; CCT7, chaperonin containing TCP-1 subunit eta; CT, C-terminal tail; DAPI, 4′,6-diamidino-2-phenylindole; DOR, delta opioid receptor; DP, prostaglandin D_2 receptor; DsiRNA, dicer-substrate short interfering RNA; ELISA, enzyme-linked immunosorbent assay; Endo Hf, endoglycosidase H; ER, endoplasmic reticulum; GPCR, G protein–coupled receptor; GST, glutathione-*S*-transferase; HA, hemagglutinin; HEK 293 cell, human embryonic kidney cell; $(His)_6$, hexahistidine; Hsp70, 70-kDa heat shock protein; ICL, intracellular loop; IgG, immunoglobulin G; MOR, mu opioid receptor; MYC, c-myc epitope; ns, nonsignificant; PBS, phosphate-buffered saline; SA, signal anchor; SRP, signal recognition particle; TBS, Tris-buffered saline; TCP-1, tailless complex protein 1; TPα, thromboxane A_2 receptor α-isoform; TPβ, thromboxane A_2 receptor β-isoform; TRiC, TCP-1 ring complex; VHL, von Hippel-Lindau.

INTRODUCTION

G protein–coupled receptors (GPCRs) form the largest and one of the most-studied families of cell-surface proteins. They respond to a vast array of cellular mediators, including hormones, neurotransmitters, lipids, nucleotides, peptides, ions, and photons. GPCRs have one of the widest therapeutic ranges and were estimated to be the targets of more than 30% of all marketed drugs (Jacoby *et al.*, 2006; Salon *et al.*, 2011). To be functional, these receptors must be correctly folded and transported to the proper location, usually the plasma membrane, in order to be activated by their respective ligands. Their seven-transmembrane structure with an extracellular N-terminus, alternating intra- and extracellular loops, and an intracellular C-terminus renders folding of GPCRs a complex process (Tao and Conn, 2014). Failure to achieve correct folding results in their retrotranslocation, ubiquitination, and endoplasmic reticulum (ER)-associated degradation (Conn and Ulloa-Aguirre, 2011). Dysregulation of GPCR folding, trafficking, and signaling contributes to

a number of pathophysiological processes (Belmonte and Blaxall, 2011; Conn and Ulloa-Aguirre, 2011; Vassart and Costagliola, 2011; Lappano and Maggiolini, 2012). Given the importance of these receptors, it is critical to understand the mechanisms that regulate their correct expression, folding, and export as nascent polypeptides, which, despite an increasing number of studies in this field of research, remain poorly characterized.

Secreted and membrane proteins possessing an N-terminal signal peptide are recognized by the signal recognition particle (SRP), leading to the cotranslational insertion of the polypeptides directly in the ER membrane through a translocon-dependent mechanism. Only 5–10% of known GPCRs contain a signal peptide that leads to their direct insertion into the ER membrane (Schülein *et al.*, 2012). Subsequent folding, posttranslational modifications, and trafficking are controlled by ER-resident proteins and chaperones (Roux and Cottrell, 2014). However, little is known regarding what happens to the majority of GPCRs that do not contain signal sequences in their N-termini. Studies have shown that transmembrane segments of GPCRs can act as signal anchor (SA) sequences and be recognized by the SRP, but it remains unclear how and when such recognition occurs (Audigier *et al.*, 1987; Schülein *et al.*, 2012). Unlike the signal peptide, the SA is not cleaved after translocon-mediated insertion into the ER. Since translation of membrane proteins lacking a signal peptide begins in the cytosol, the SRP has a very short window of time to bind the translating ribosome and recognize the SA, because their interaction is inversely proportional to the polypeptide length (Berndt *et al.*, 2009). If the SRP is unable to bind the SA, the synthesized protein is exposed to the cytosolic environment, which can result in aggregation and misfolding (White *et al.*, 2010). To prevent this from happening, eukaryotic cells possess chaperone proteins that assist the folding process of nascent polypeptides, maintaining them in an intermediate state of folding competence for posttranslational translocation in subcellular compartments. Two complexes of chaperone proteins have been identified to interact posttranslationally with near nascent proteins and seem to affect their translocation into the ER. The first is the well-known 70-kDa heat shock protein (Hsp70) system, and the second is the tailless complex polypeptide 1 (TCP-1), a group II chaperonin, also known as the CCT/TCP-1 ring complex (TRiC complex; Deshaies *et al.*, 1988; Plath and Rapoport, 2000). The exact sequence of posttranslational events leading to ER insertion is not fully understood, but studies have proposed a three-step process. First, the nascent peptide emerging from ribosomes is able to interact with the nascent polypeptide-associated complex or the SRP, which both regulate translational flux (Kirstein-Miles *et al.*, 2013). However, once translation is completed, these proteins are no longer able to bind the polypeptide. Second, Hsp70 and/or CCT/TRiC complexes bind polypeptides to maintain a translocable state by preventing premature folding, misfolding, and aggregation (Melville *et al.*, 2003; Cuéllar *et al.*, 2008). Third, ER-membrane insertion is mediated by the translocon, which strips away the cytosolic chaperones. This process is called the posttranslational translocation pathway (Ngosuwan *et al.*, 2003).

CCT/TRiC is a large cytosolic chaperonin complex of ~900 kDa composed of two hetero-oligomeric stacked rings able to interact with nascent polypeptides, which mediates protein folding in an ATP-dependent manner and prevents aggregation in eukaryotes (Knee *et al.*, 2013). Each ring consists of eight different subunits (CCT1 to CCT8) that share ~30% sequence homology, particularly in their equatorial domains, which mediate interactions between subunits (Valpuesta *et al.*, 2002). CCT/TRiC was originally characterized for its role in the folding of α-actin (Llorca *et al.*, 1999). In recent years, the list of identified substrates for this complex has grown in both number and variety. For example, it has been shown that CCT/TRiC can bind and/or help the folding of different WD-repeat proteins like the G-protein β subunits (Plimpton *et al.*, 2015), STAT3 (Kasembeli *et al.*, 2014), the von Hippel-Lindau (VHL) protein (Melville *et al.*, 2003), and even membrane proteins such as the peroxisome membrane protein Pmp22p (Pause *et al.*, 1997) and the cell-surface receptor LOX-1 (Bakthavatsalam *et al.*, 2014). The central cavity formed by the two stacked rings protects the newly synthesized polypeptide against aggregation in the crowded environment of the cytosol. This large cavity can accommodate a wide range of protein sizes from 20 to 200 kDa (Dekker *et al.*, 2008). It was shown that CCT/TRiC can cotranslationally bind nascent polypeptides exposing at least 50 amino acids outside of the ribosome exit channel, but this number can vary between the different substrates (McCallum *et al.*, 2000).

Here we report a direct and functional interaction between GPCRs and the chaperonin containing TCP-1 subunit eta (CCT7). We provide evidence that CCT7 is involved in preventing aggregation of GPCRs and in regulating their expression, maturation, and transport to the cell surface. To our knowledge, this is the first demonstration of a functional interaction between GPCRs and the CCT/TRiC complex.

RESULTS

CCT7 interacts with the β-isoform of thromboxane A_2 receptor (TPβ) and β_2-adrenergic receptor (β_2AR)

A yeast two-hybrid screen was performed using the C-terminus of TPβ as bait with a human HeLa cell MATCHMAKER cDNA library. Roughly 3×10^6 clones were screened, resulting in more than 600 positives. Approximately 200 of these clones showed strong growth on selective yeast medium (Trp^-, Leu^-, His^-, and Ade^-) and were isolated, characterized by dideoxy sequencing, and then aligned using the NCBI BLAST alignment search tool. Five independent clones covering the full-length CCT7 coding sequence were identified in this screen. As shown in Figure 1A, only yeast transformed with the pAS2.1-TPβ C-terminus and pGAD-CCT7 showed strong growth on selective Trp^-, Leu^-, His^-, and Ade^- yeast medium, indicating that CCT7 interacts with the TPβ C-terminus.

Interestingly, we also identified CCT7 as a putative interactor of the β_2AR using a gel-free proteomic approach, but the interaction and its functional consequences were not characterized (Roy *et al.*, 2013). To assess the interaction between CCT7 and both GPCRs in a cellular context, we performed immunoprecipitation experiments in HEK 293 cells transfected with pcDNA3-FLAG-β_2AR or pcDNA3-HA-TPβ and pcDNA3-CCT7–c-myc epitope (MYC). Cell lysates were incubated with FLAG-specific or hemagglutinin (HA)-specific monoclonal antibodies, and coimmunoprecipitation of CCT7 was detected by Western blot analysis using a Myc-specific antibody. CCT7 coimmunoprecipitated with both receptors (Figure 1, B and C), confirming that CCT7 forms a complex with either TPβ or β_2AR in cells. Importantly, our data further show that the interaction can be detected endogenously. Indeed, HEK 293 cell lysates were incubated with CCT7-specific or nonspecific goat antibodies and coimmunoprecipitation of endogenous β_2AR was detected by Western blot analysis using a β_2AR-specific antibody. Endogenous β_2AR was coimmunoprecipitated only when endogenous CCT7 was immunoprecipitated (Figure 1D).

Depletion of CCT7 impairs β_2AR and TPβ total and cell-surface expression

To characterize the functional role of CCT7 interactions with β_2AR and TPβ, we first investigated the effect of CCT7 depletion on total

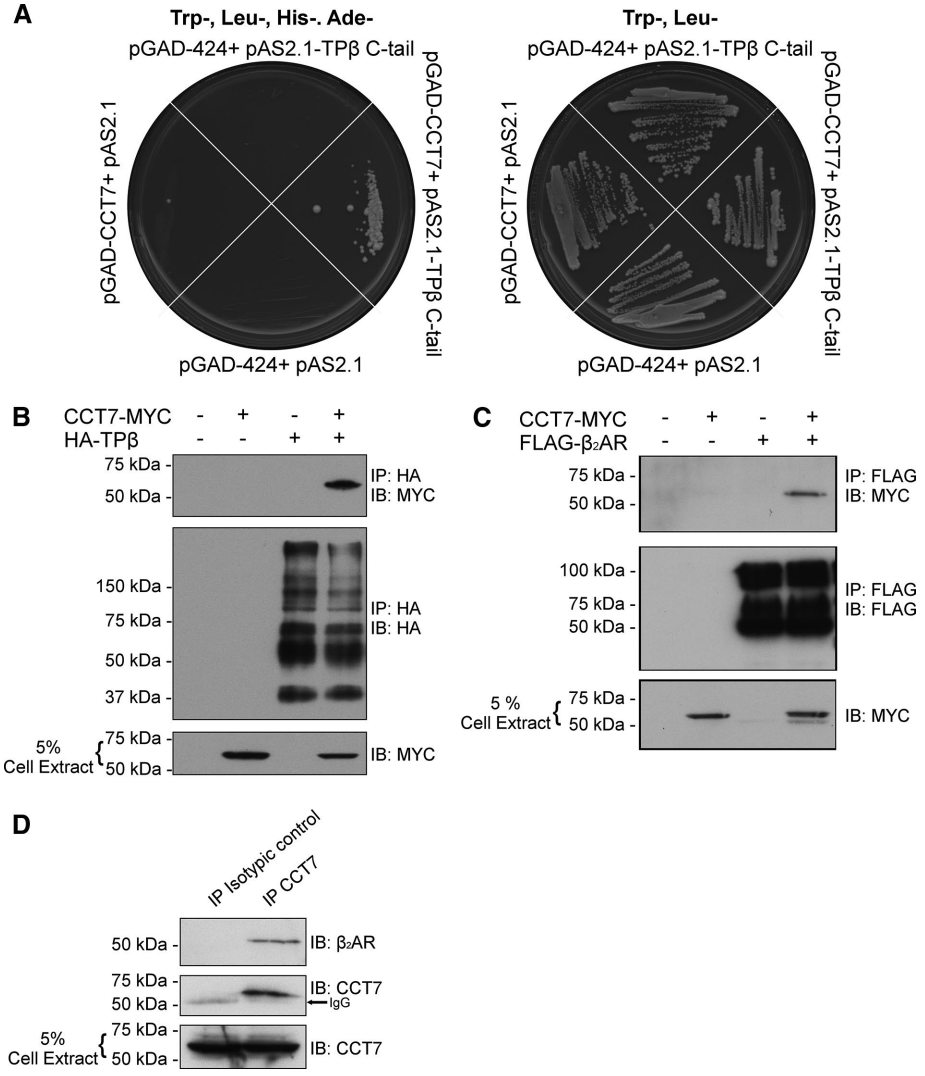

FIGURE 1: TPβ and β_2AR interact with CCT7. (A) A yeast two-hybrid screen was performed using the TPβ C-terminus portion as bait on a human HeLa cell MATCHMAKER cDNA library. The interaction between CCT7 and the TPβ C-terminus was confirmed by the use of the selective yeast medium Trp^-, Leu^-, His^-, and Ade^-. (B) Lysates of HEK 293 cells transiently expressing HA-TPβ and CCT7-MYC alone or together were immunoprecipitated with HA-specific monoclonal antibody, and immunoblotting was performed with HA-specific HRP and MYC-specific HRP-conjugated antibodies. (C) Lysates of HEK 293 cells transiently expressing FLAG-β_2AR and CCT7-MYC alone or together were immunoprecipitated with FLAG-specific monoclonal antibody, and immunoblotting was performed with Flag-specific polyclonal and MYC-specific HRP-conjugated antibodies. (D) HEK 293 cells lysates were incubated with either nonspecific goat or CCT7-specific goat polyclonal antibodies, and immunoblotting was performed using the same CCT7-specific and a β_2AR-specific rabbit polyclonal antibody. All blots shown are representative of at least three independent experiments. IB, immunoblotting; IP, immunoprecipitation.

expression of the receptors by Western blot. HEK 293 cells stably expressing HA-β_2AR or HA-TPβ were transfected with control or CCT7 dicer-substrate short interfering RNAs (DsiRNAs). Figure 2, A and B, shows that the partial depletion of CCT7 leads to decreased total protein expression of both receptors. Densitometry analyses of multiple independent experiments revealed that CCT7 depletion resulted in a loss of 42 and 37% in total receptor expression for TPβ and β_2AR, respectively (Figure 2, C and D). We then assessed the importance of CCT7 expression on the cell-surface expression of β_2AR, TPβ, and thromboxane A_2 receptor α-isoform (TPα), a shorter isoform of TP compared to TPβ generated by alternative splicing of the receptor C-terminus (Raychowdhury *et al.*, 1994). HEK 293 cells expressing HA-tagged TPβ, TPα, or β_2AR were transfected with control or CCT7 DsiRNAs and receptor cell-surface expression was measured by enzyme-linked immunosorbent assay (ELISA). CCT7 depletion significantly decreased TPβ cell-surface expression by 50% (Figure 2E), whereas cell-surface expression of TPα and β_2AR was less affected, with reductions of 30 and 22%, respectively (Figure 2, F and G).

In mammals, nascent polypeptides emerging from ribosomes are bound by Hsc70, which operates in concert with the CCT/TRiC complex in the folding of polypeptides. Alternatively, polypeptides can be passed to Hsp90 (Young *et al.*, 2004). In an attempt to address why CCT7 depletion affected the cell-surface expression of TPβ more significantly than that of β_2AR, we compared the ability of both receptors to interact with Hsp90. Lysates of HEK 293 cells expressing FLAG-β_2AR or FLAG-TPβ and HA-Hsp90 were immunoprecipitated with a Flag-specific antibody, and Hsp90 interaction was studied by Western blot analysis with an HA-specific monoclonal antibody (Figure 2H). Interestingly, significantly more Hsp90 protein coimmunoprecipitated with β_2AR than with TPβ.

CCT7 colocalizes with β_2AR and TPβ and regulates their intracellular distribution

Confocal microscopy was performed in HEK 293 cells stably expressing HA-β_2AR or HA-TPβ that were transfected or not with control or CCT7 DsiRNAs and labeled with HA- and CCT7-specific antibodies. Figure 3, Ab and Bb, shows the levels of nonspecific secondary antibody–associated staining compared with the labeling obtained with the CCT7-specific antibody (Figure 3, Af and Bf). Endogenous CCT7 displayed cytosolic and nuclear localization in control DsiRNA-treated cells. HA-TPβ was distributed at the plasma membrane and in intracellular compartments in nontreated and control DsiRNA-transfected cells (Figure 3A, c and g), as we reported before (Thériault *et al.*, 2004; Parent *et al.*, 2009). Under the same conditions, HA-β_2AR was primarily localized to the plasma membrane with some intracellular labeling (Figure 3B, c and g). Analysis of merged images revealed that CCT7 mainly colocalized with both receptors in the juxtanuclear region of the cell (Figure 3, Ah and Bh). Transfection of CCT7 DsiRNAs significantly diminished expression of endogenous CCT7 (Figure 3, Aj and Bj) and caused a marked redistribution of both receptors to an intracellular and juxtanuclear localization, which was more pronounced for HA-TPβ (Figure 3, Ak and Bk), in agreement with data obtained in receptor cell-surface expression experiments (Figure 2, E and G). Depletion of CCT7 also appeared to decrease receptor-associated fluorescence for both

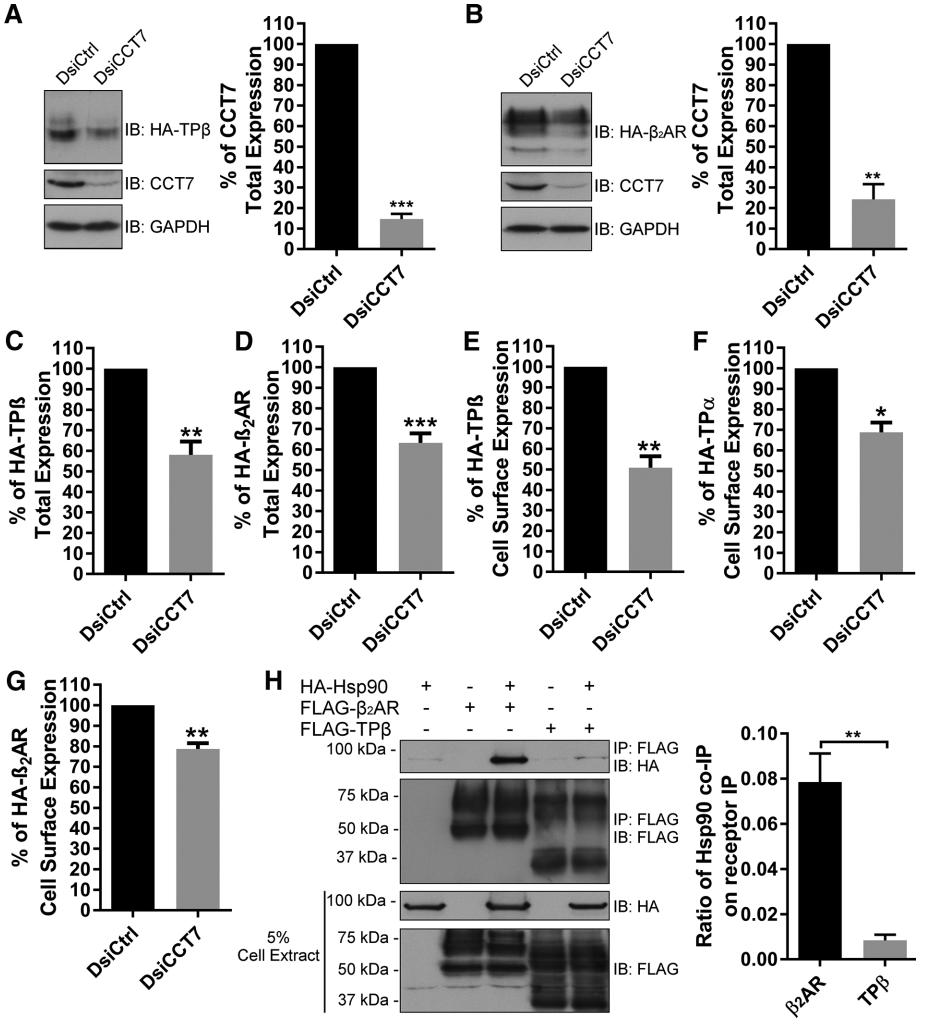

FIGURE 2: CCT7 depletion impairs TPβ and β_2AR total and cell-surface expression. HEK 293 cells stably expressing HA-TPβ (A) or HA-β_2AR (B) were transfected with control DsiRNA (DsiCtrl) or CCT7 DsiRNA (DsiCCT7), and lysates were immunoblotted with HA-specific HRP-conjugated, CCT7-specific and GAPDH-specific antibodies. Densitometry was performed on the Western blots to quantify relative expression of HA-TPβ (C) and HA-β_2AR (D) in cells treated with CCT7 DsiRNA compared with control DsiRNA-transfected cells (100%) and normalized to GAPDH expression. Densitometry was performed using ImageJ software, and the results are presented as mean ± SD of at least four independent experiments. Cell-surface receptor expression was measured in HEK 293 cells expressing HA-TPβ (E), HA-TPα (F), or HA-β_2AR (G) transfected with control or CCT7 DsiRNAs by ELISA using a monoclonal HA-specific antibody as described in *Materials and Methods*. Results are shown as a percentage of cell-surface receptor expression when cells were transfected with CCT7 DsiRNA compared with control DsiRNA condition (100%). (H) Lysates of HEK 293 cells transiently expressing FLAG-TPβ or FLAG-β_2AR and HA-Hsp90 alone or together were immunoprecipitated with FLAG-specific monoclonal antibody, and immunoblotting was performed with FLAG-specific polyclonal and HA-specific HRP-conjugated antibodies. Densitometry on Western blots of five independent experiments are reported in the graphic and expressed as a ratio of HSP90 co-IP on receptors IP. Results are presented as mean ± SEM of at least four independent experiments.
IB, immunoblotting; IP, immunoprecipitation.

receptors, also supporting our findings from Western blot analyses (Figure 2, A and B).

CCT7 depletion induces accumulation of misfolded receptors in intracellular aggregates

Because the distribution of the receptors was reminiscent of Golgi localization in cells transfected with CCT7 DsiRNAs, we performed colocalization studies between TPβ and GM130, a Golgi marker, in CCT7-depleted HEK 293 cells (Figure 4A). Partial colocalization was observed between the receptor and GM130 (Figure 4Ad). The relocalization of misfolded proteins to a juxtanuclear localization and a spatial overlap with the Golgi apparatus have been demonstrated to be associated with the formation of aggresomes (Johnston *et al.*, 1998; García-Mata *et al.*, 1999; Salemi *et al.*, 2014). Aggresomes are made up of aggregated inclusion bodies and misfolded proteins (Watanabe *et al.*, 2012). Given the function of CCT7 in protein folding, we reasoned that the receptors could be found in aggresomes in CCT7-depleted cells. Confocal microscopy was performed as above in HEK 293 cells stably expressing HA-TPβ or HA-β_2AR transfected with control or CCT7 DsiRNAs (Figure 4, B and D). Cells were also stained with a probe, the PROTEOSTAT dye, designed to detect aggresomes by recognition of inclusion bodies and misfolded proteins. Low levels of colocalization were detected between the receptors and aggresomes under control conditions represented by low Mander's colocalization coefficients of 0.03 and 0.01 for TPβ and β_2AR, respectively (Figure 4, C and E). However, CCT7 depletion resulted in increased colocalization of both receptors with aggresomes in a juxtanuclear region (Figure 4, Bf and Df). This was more drastic for TPβ than for β_2AR, as indicated by Mander's colocalization coefficients in CCT7-depleted cells of 0.84 and 0.30 for TPβ and β_2AR, respectively (Figure 4, C and E). These results indicate that CCT7 depletion induced an accumulation of misfolded TPβ and β_2AR in intracellular aggregates, notably more pronounced for the former. It is also interesting to observe an overall augmentation of the aggresome staining across the cytosol of CCT7-depleted cells compared with the control (Figure 4, Be and De). This is probably caused by the detection, by the PROTEOSTAT dye, of other broadly distributed misfolded proteins.

Determination of the CCT7-binding domain on β_2AR and TPβ

To establish whether or not the interaction of CCT7 with receptors could be direct, and if so to determine its binding domains on β_2AR and TPβ, we performed in vitro binding assays with purified forms of recombinant intracellular loops (ICL) or C-termini (CT) of both receptors fused to glutathione S-transferase (GST) along with purified CCT7-MYC fused with a hexa-His tag (His_6-CCT7-MYC). We also investigated whether CCT7 interacted with the C-terminus of TPα, a C-terminal spliced isoform of TP that shares its first 328 amino acids with TPβ. Results presented in Figure 5, A and B, show a binding reaction between His_6-CCT7-MYC bound to nickel–nitrilotriacetic acid–agarose beads and

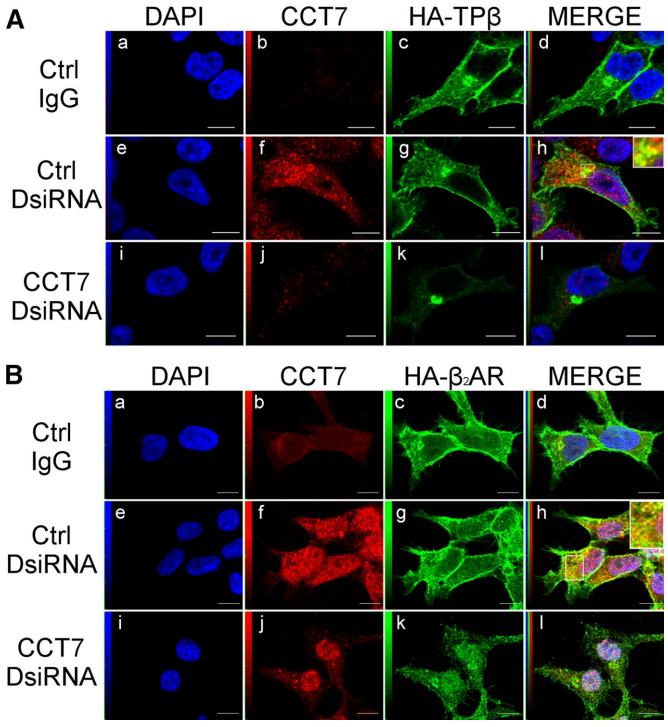

FIGURE 3: CCT7 colocalizes with TPβ and β_2AR and regulates their intracellular distribution. Confocal microscopy was performed on HEK 293 cells stably expressing HA-TPβ (A) or HA-β_2AR (B) treated with control or CCT7 DsiRNAs. Cells were fixed, permeabilized, and labeled with goat nonspecific IgG as a control, goat anti-CCT7 IgG, and mouse anti-HA IgG. Secondary antibodies used were Alexa Fluor 488–conjugated anti-mouse IgG and Texas red–conjugated anti-goat IgG. Cells were then stained with 4′,6-diamidino-2-phenylindole (DAPI) to visualize nuclei (a, e, and i). The fourth panel on the right represents a merged image of the blue, green, and red signals where the areas with high degree of colocalization between green-labeled receptors (c, g, and k) and red-labeled CCT7 (f and j) appear yellow (h). Approximately 88% of the 250 CCT7-depleted cells observed showed juxtanuclear accumulation of TPβ compared with 7% of the 250 control cells. Images shown are single confocal slices representative of at least four independent experiments and more than 250 observed cells. Scale bars: 10 μm.

GST-TPβ-CT, GST-β_2AR-CT, and GST-ICL3 of both receptors. No significant interaction was observed with other intracellular loops or with GST-TPα-CT (Figure 5A). These results indicate that CCT7 can interact directly with the C-terminus and the third intracellular loop of β_2AR and TPβ. However, no interaction was detected between CCT7 and the TPα C-terminus. It thus appeared that the CCT7 interaction with the TPβ C-terminus occurs on sequences that differ between the TPβ and TPα C-termini (Figure 6A). To elucidate the region of the TPβ C-terminus involved in interacting with CCT7, we used progressive HA-tagged C-terminal deletion mutant constructs of the receptor to perform CCT7 coimmunoprecipitation experiments in HEK 293 cells. As shown in Figure 6B, the majority of the CCT7 coimmunoprecipitation was lost with the HA-TPβ 328-Stop mutant compared with the wild-type receptor but recovered nearly to wild-type receptor levels with the HA-TPβ 337-Stop mutant, as supported by densitometry analysis of four independent experiments. These data suggest that determinants found between residues 328 and 337 in the TPβ C-terminus are essential for the interaction with CCT7 in a cellular context. Amino acids in the ICL3 may participate in the CCT7 interaction but are not sufficient, as both TPα and the TPβ 328-Stop mutant failed to coimmunoprecipitate CCT7.

Trp^{334} of TPβ is involved in the interaction with CCT7

We compared the amino acid sequences between residues 328 and 337 of TPα and TPβ (Figure 6A), based on the above results. Because the CCT complex can interact with bulky hydrophobic amino acids in its client proteins (Spiess *et al.*, 2006), the Trp^{334} residue of TPβ and Gln^{333} of TPα particularly stood out as interesting differences between the two receptor forms. We thus decided to exchange the residues between the two receptors to generate the TPβ W334Q and TPα Q333W mutants and studied whether this altered the CCT7-binding properties of the receptors. CCT7 coimmunoprecipitation experiments with these HA-tagged receptor mutants in HEK 293 cells revealed that the TPβ W334Q mutation severely impaired the interaction with CCT7 by ~85% compared with wild-type TPβ (Figure 6C, lane 6 vs. lane 4, and densitometry, right panel). Interestingly, the reverse mutation in TPα (TPα Q333W) strongly promoted the interaction with CCT7 compared with wild-type TPα to levels comparable to wild-type TPβ (Figure 6C, lane 10 vs. lane 8, and densitometry, right panel). Taken together, these data show that Trp^{334} of TPβ is a critical determinant in the interaction with CCT7.

Role of Trp^{334} in TPβ maturation

Closer observation by Western blot analysis of the migration patterns of the TPβ W334Q and TPα Q333W mutants from cell lysates revealed that they were different from their respective wild-type counterparts. Figure 7A shows that wild-type HA-TPβ was detected as a major form at ~40 kDa and a minor form at ~70 kDa. In contrast, HA-TPβ W334Q displayed the opposite pattern, with minor and major forms at ~40 and ~70 kDa, respectively. The latter was reminiscent of the expression pattern shown by wild-type HA-TPα (Figure 7B), which migrated as a prominent form in the ~50–55 kDa range and as a minor form at ~35 kDa. On the other hand, the TPα Q333W mutation induced a redistribution of the higher molecular form of the receptor toward the lower ~35 kDa form, analogous to the distribution of the wild-type HA-TPβ.

We previously reported that the TPβ ~70 kDa and TPα ~50-55 kDa forms corresponded to glycosylated dimers of the receptors measured using treatment with peptide N-glycosidase F, which removes all types of N-linked oligosaccharides from glycoproteins (Laroche *et al.*, 2005). Here we further analyzed the glycosylation patterns of TP isoforms with endoglycosidase H (Endo Hf), an N-glycosidase that selectively removes unprocessed high mannose–type N-linked oligosaccharides present on ER-resident glycoproteins. Glycosylated TP receptor proteins that have undergone trimming in the Golgi will be resistant to Endo Hf treatment. Lysates of HEK 293 cells expressing HA-TPβ or HA-TPα were treated with Endo Hf and then analyzed by Western blot. As shown in Figure 7C, the larger HA-TPβ ~70 kDa and TPα ~50-55 kDa forms were predominantly unaltered, whereas the lower forms of the receptors were reduced in size upon Endo Hf treatment. Altogether our present data, along with our earlier results (Laroche *et al.*, 2005), indicate that the lower molecular weight bands of TPβ and TPα are immature monomeric forms of the receptors present in the ER. On the other hand, the higher molecular weight Endo Hf–resistant forms represent dimeric TP receptors that have undergone complex glycosylation in the Golgi. Consistent with this, our results suggest that the HA-TPβ W334Q mutation promoted receptor maturation through the Golgi toward a glycosylated receptor dimer (Figure 7A). In contrast, the

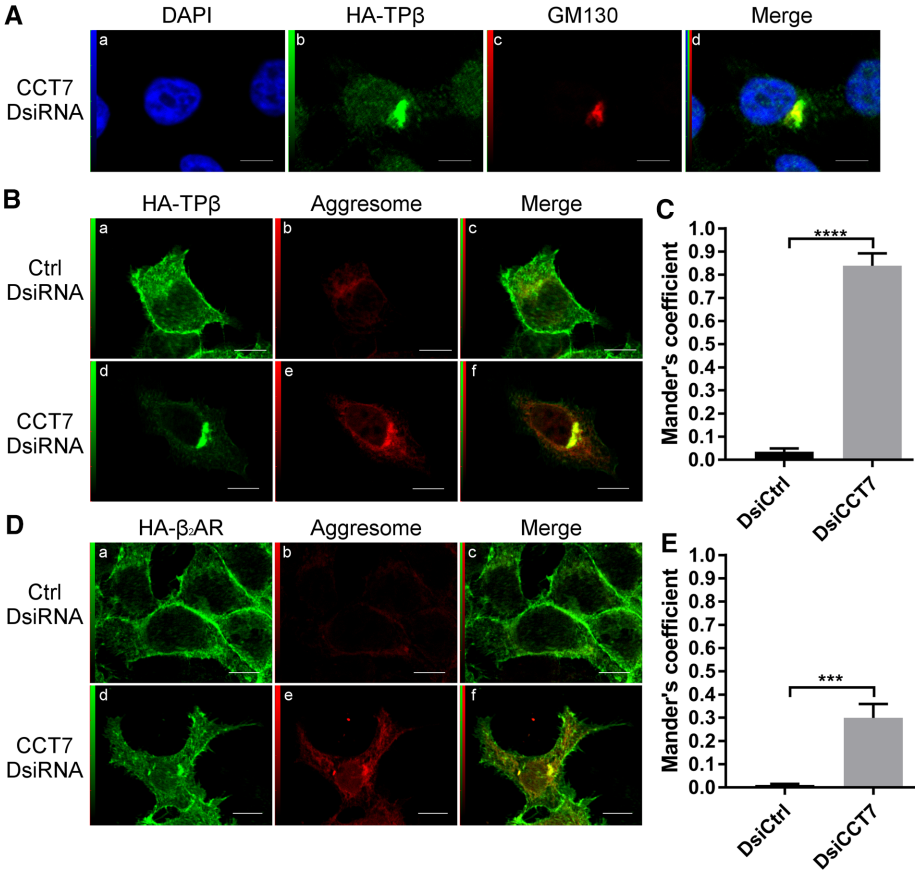

FIGURE 4: CCT7 depletion causes redistribution of receptors in aggresomes. (A) HEK 293 cells stably expressing HA-TPβ transfected with CCT7 DsiRNA were fixed, permeabilized, and labeled with a rabbit anti-HA IgG and a mouse anti-GM130. Alexa Fluor 488–conjugated anti-rabbit IgG and Alexa Fluor 633–conjugated anti-mouse IgG were used as secondary antibodies. The fourth panel (d) represents a merge image of the blue (a), green (b), and red (c) signals. High degree of colocalization between the red and green signals appears in yellow. HEK 293 cells stably expressing HA-TPβ (B) or HA-β_2AR (D) were treated with control or CCT7 DsiRNAs. The cells were fixed, permeabilized, and labeled with mouse anti-HA IgG and stained with PROTEOSTAT aggresome dye. We used Alexa Fluor 633–conjugated anti-mouse IgG as secondary antibody. The third image on the right represents a merged image (c and f) of the green and red signals where the areas with high degree of colocalization between the green signal of the receptors (a and d) and red signal of the aggresome (b and e) appear yellow. Scale bars: 10 μm. Images shown are single confocal slices representative of at least four independent experiments and more than 250 observed cells. (C, E) Mander's colocalization coefficients represent the ratio of the green signal of the receptors overlapping the red signal of the aggresome and were calculated from at least 100 cells per condition. Results are presented as mean ± SEM.

TPα Q333W receptor displayed impaired maturation compared with wild-type TPα (Figure 7B).

Using ELISAs in HEK 293 cells, we then evaluated whether the effects of the TPβ W334Q and TPα Q333W substitutions on receptor maturation were reflected in receptor cell-surface expression. Compared with wild-type HA-TPβ, cell-surface expression of HA-TPβ W334Q was increased by more than 200% to reach similar levels as HA-TPα (Figure 7D). Conversely, HA-TPα Q333W detection at the cell membrane was reduced by 50% compared with wild-type HA-TPα (115 vs. 239%), akin to wild-type HA-TPβ expression levels. The effect of the TPβ W334Q mutation on cell-surface expression of the receptor was also studied by confocal microscopy. HEK 293 cells transiently expressing HA-TPβ or HA-TPβ W334Q were labeled with an HA-specific antibody to visualize the receptors and with a CCT7-specific antibody to detect endogenous CCT7 (Figure 8A). As we reported before, wild-type TPβ exhibited plasma membrane staining accompanied by strong intracellular localization (Figure 8Ac). On the other hand, the TPβ W334Q mutant displayed robust membrane localization (Figure 7Ag). Quantification of receptor immunofluorescence was carried out on 100 cells for each receptor construct. Figure 8B shows that 25% of wild-type TPβ immunofluorescence was found at the plasma membrane, compared with 55% for the TPβ W334Q mutant, a roughly twofold difference, confirming our cell-surface expression data obtained by ELISA (Figure 7D). We also observed that TPβ colocalized more significantly with CCT7 than did the TPβ W334Q mutant (Figure 8A, d and h). Quantification of CCT7 colocalization with the two receptor constructs revealed Mander's colocalization coefficients of 0.43 for TPβ and 0.12 for TPβ W334Q (Figure 8C). This marked decrease in CCT7 colocalization with the TPβ W334Q mutant is in line with the virtual lack of detectable coimmunoprecipitation between the two proteins (Figure 6C).

Next we assessed the effect of CCT7 depletion on the colocalization of the TPβ W334Q mutant with the aggresome. Confocal microscopy experiments showed that the receptor mutant, in the presence of CCT7 DsiRNAs, was readily detected at the cell surface (Figure 9Ad) but also redistributed to the aggresome (Figure 9Af). Quantification of the colocalization between the TPβ W334Q mutant and the aggresome yielded a Mander's coefficient of colocalization of 0.51 when CCT7 was depleted compared with 0.10 when the cells were transfected with control DsiRNAs (Figure 9B). These results indicate that the receptor mutant is still affected by CCT7 depletion in terms of redistribution to the aggresome but in a less drastic way than was wild-type TPβ (Figure 4, B and C, Mander's coefficient of 0.84). Taken together, our results indicate that Trp^{334} of TPβ interacts with CCT7 and plays an important role in the maturation and cell-surface expression of the receptor.

CCT7 interacts with other GPCRs

Finally, knowing that CCT7 can interact with the β_2AR and TPβ but not with TPα, we wanted to extend our coimmunoprecipitation studies to a few other GPCRs. Lysates of HEK 293 cells transiently expressing HA-tagged rat μ-opioid receptor (MOR; Figure 10A), FLAG-tagged rat δ-opioid receptor (DOR; Figure 10B), or FLAG-tagged prostaglandin D_2 receptor (DP; Figure 10C) with or without CCT7-MYC were incubated with HA- or FLAG-specific antibodies. Coimmunoprecipitation of CCT7 was detected by Western blot analysis using a Myc-specific antibody. Coimmunoprecipitation of CCT7 was observed with each of the three receptors. Our data suggest that CCT7 can interact with various GPCRs, but not all, and that

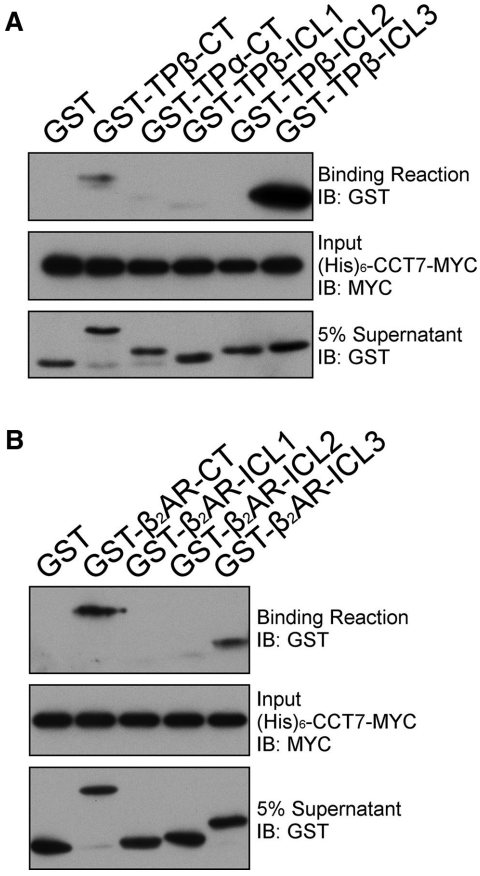

FIGURE 5: Identification of the CCT7-binding domains on TPβ and β_2AR. (A) His pull-down assays were carried out using purified hexahistidine $(His)_6$-CCT7-MYC bound to nickel–nitrilotriacetic acid–agarose beads incubated with purified GST or GST fused to the TP C-termini (GST-TPβ-CT and GST-TPα-CT) and intracellular loops (GST-TPβ-ICL). (B) His pull-down assays were carried out using purified $(His)_6$-CCT7-MYC bound to nickel–nitrilotriacetic acid–agarose beads incubated with purified GST or GST fused to the β_2AR C-terminus (GST-β_2AR-CT) and intracellular loops (GST-β_2AR-ICL). The binding of GST-fusion proteins in A and B was detected by immunoblotting with a GST-specific HRP-conjugated antibody, and the $(His)_6$-CCT7-MYC present in the binding reactions was detected with a MYC-specific HRP-conjugated antibody. Blots shown are representative of at least five independent experiments.

it can display specificity at the interaction and functional levels between different receptors.

DISCUSSION

GPCRs contain seven highly hydrophobic α-helical membrane-spanning domains and are particularly prone to misfolding and aggregation (Achour *et al.*, 2008). While an increasing number of studies have described the chaperones and other associated proteins involved in GPCR folding and maturation from the ER to the plasma membrane (Tao and Conn, 2014), our knowledge of the chaperone proteins that interact with nascent GPCR polypeptides remains limited. In the present study, we have characterized functional interactions between two GPCRs and CCT7, a subunit of the CCT/TRiC complex that binds to nascent polypeptides (McCallum *et al.*, 2000).

CCT/TRiC is distinguished from other chaperones by its unique ring-shaped structure, which forms a central cavity that serves as a folding chamber for substrates (Yam *et al.*, 2008). Bioinformatics analysis of the CCT/TRiC substrates noted that the CCT/TRiC interactome is enriched in large, hydrophobic proteins with intricate topologies predicted to be slow folding and aggregation prone and belonging to oligomeric protein complexes. On the other hand, CCT/TRiC could fold monomeric subunits and maintain them in an assembly-competent state until association with oligomeric partners (Yam *et al.*, 2008). Here we provide evidence that the CCT/TRiC chaperonins prevent aggregation and participate in the folding and maturation of the complex seven-transmembrane GPCR proteins known to form oligomeric structures between receptor units and with signaling partners during their biogenesis (Dupré and Hébert, 2006; Dupré *et al.*, 2006).

We first identified the interaction between CCT7 and TPβ by yeast two-hybrid screening with the C-terminus of the receptor. We also detected all of the eight CCT subunits as potential β_2AR-binding partners in liquid chromatography–tandem mass spectrometry proteomics studies (Roy *et al.*, 2013). Our data showed that TPβ and β_2AR can interact directly with CCT7 through their third intracellular loops and their C-termini. The interaction was confirmed by coimmunoprecipitation experiments in a cellular context in overexpression settings for both receptors but notably also between endogenous CCT7 and β_2AR proteins. Further analysis also showed that CCT7 coimmunoprecipitated in HEK 293 cells with other GPCRs, such as the prostaglandin D_2 DP1, and the μ- and δ-opioid receptors, suggesting that CCT7 may be involved in a general mechanism of GPCR biogenesis.

TPβ displays prominent intracellular localization in our system, which is consistent with the fact that it is prone to ER retention and ER-associated degradation as shown previously by us and others (Parent *et al.*, 2008; Ball *et al.*, 2010). Depletion of CCT7 resulted in lower total and cell-surface expression for both TPβ and β_2AR. It also caused redistribution of the receptors to aggresomes, drastically in the case of TPβ. This indicates that CCT7 is involved in preventing aggregation and degradation of the receptors. Of note, it was shown that mutation of CCT7 in yeast caused the VHL protein to accumulate in juxtanuclear aggregates (Amit *et al.*, 2010), similar to what we observed for the receptors in our study. It is also interesting that the misfolded GPCR rhodopsin P23H mutant, associated with autosomal-dominant retinitis pigmentosa, also accumulates in aggresomes and is ubiquitinated and degraded by the proteasome (Saliba *et al.*, 2002), further supporting the notion that inappropriately folded GPCRs are targeted to aggresomes. The receptors in CCT7-depleted cells colocalized with a subfraction of the misfolded proteins stained by the PROTEOSTAT aggresome dye, with a juxtanuclear localization that overlapped partially with the Golgi. Aggregated inclusion bodies and misfolded proteins accumulate in aggresomes (Watanabe *et al.*, 2012). This aggregation process is more likely to occur cotranslationally while hundreds of nascent polypeptides chains emerge from the polysomes at the same time in a single localization leading to the improper folding (Garcia-Mata *et al.*, 2002). The aggresomal particles are then transported toward the microtubule organizing center via dynein to be sequestered in a large single structure called the aggresome (García-Mata *et al.*, 1999). This juxtanuclear sequestration is a nontoxic cellular response to misfolded proteins and is known to help the recruitment of various chaperones such as Hsc70, Hsp90, and even the CCT/TRiC complex as an ultimate resort for refolding (García-Mata *et al.*, 1999; Wigley *et al.*, 1999). This further supports our data showing that the β_2AR, and particularly TPβ, accumulate in aggresomes in CCT7-depleted cells. Proteins that cannot be refolded will enter both lysosomal and proteasomal degradation pathways (Garcia-Mata *et al.*, 2002).

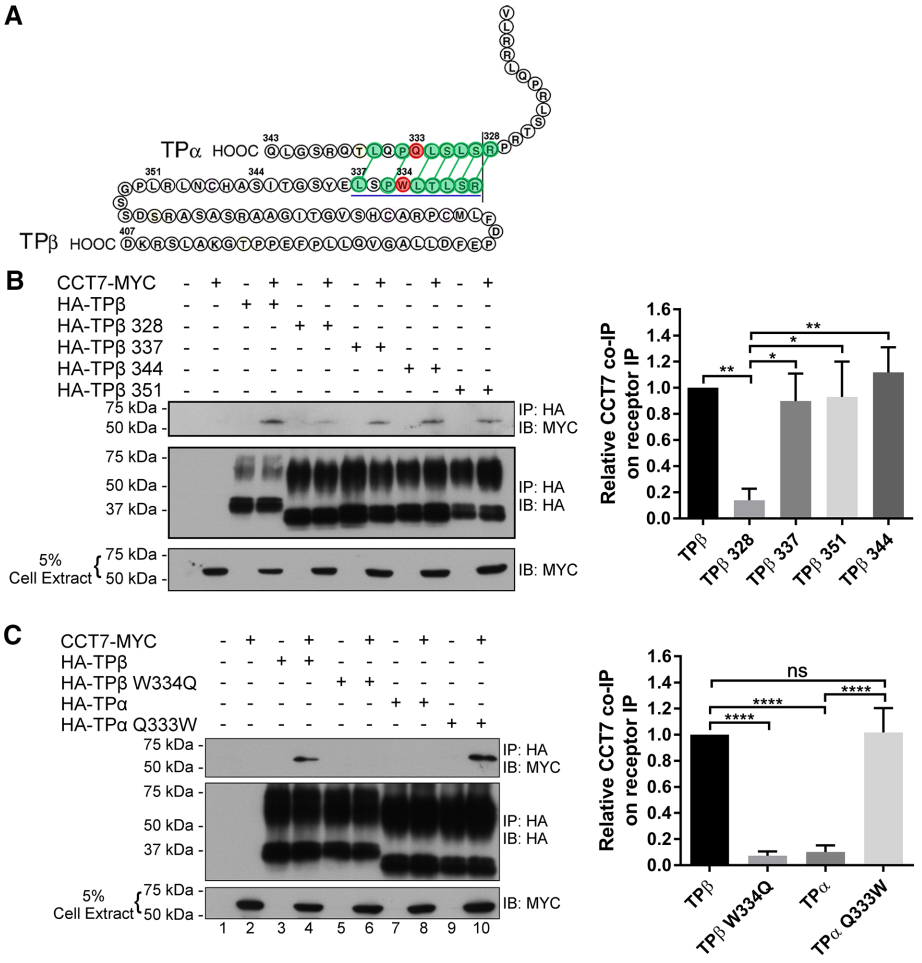

FIGURE 6: TPβ Trp^{334} is a major determinant for CCT7 interaction. (A) Schematic representation of TPβ and TPα C-termini. The TPβ region important for CCT7 interaction is underlined in blue. The green, linked amino acids represent residues showing similarity or identity between TPβ and TPα. Shown in red are TPβ Trp^{334} and TPα Gln^{333}. (B) Lysates of HEK 293 cells transiently expressing the indicated HA-TPβ constructs alone or with CCT7-MYC were immunoprecipitated with a HA-specific monoclonal antibody and analyzed by immunoblotting with MYC- and HA-specific HRP-conjugated antibodies. HA-TPβ 328, 337, 344, and 351 indicate that a stop codon was introduced after the corresponding amino acids. Densitometry on Western blots of four independent experiments are reported in the graphic and expressed as a relative ratio of CCT7 co-IP on receptors IP. (C) Lysates of HEK 293 cells transiently expressing HA-TPβ, HA-TPβ W334Q, HA-TPα, or HA-TPα Q333W alone or with CCT7-MYC were immunoprecipitated with a HA-specific monoclonal antibody and analyzed by immunoblotting with MYC- and HA-specific HRP-conjugated antibodies. Densitometry on Western blots of five independent experiments are reported in the graphic and expressed as a relative ratio of CCT7 co-IP on receptors' IP. IB, immunoblotting; IP, immunoprecipitation.

The β_2AR was less affected than TPβ by CCT7 expression knockdown. This suggested that the β_2AR might take advantage of complementary folding pathways. Indeed, as nascent polypeptide chains emerge from ribosomes they are met by Hsc70. The latter may act together with CCT/TRiC in the folding of different polypeptides. Other newly synthesized polypeptides can fold spontaneously or be assisted by Hsc70. Alternatively, they can be passed from Hsc70 to Hsp90 for subsequent folding (Young *et al.*, 2004). Our data showed that Hsp90 coimmunoprecipitated with the β_2AR, whereas its interaction with TPβ was negligible. This indicates that nascent GPCR polypeptides can be subjected to distinct folding pathways depending on the receptor and could explain, at least in part, why the β_2AR cell-surface expression was less sensitive to CCT7 depletion than TPβ. Involvement of Hsp90 has been reported in the folding and trafficking of other GPCRs, such as the melanocortin-4 receptor (Meimaridou *et al.*, 2011), the prostaglandin D_2 receptor (Binda *et al.*, 2014), the adenosine A_2A receptor (Bergmayr *et al.*, 2013), and the α_{2c}-adrenergic receptor (Filipeanu *et al.*, 2011).

Our results demonstrated that Trp^{334} is crucial for TPβ to bind to CCT7 and that introduction of a tryptophan residue in the TPα C-terminus promoted its interaction with CCT7. Strikingly, the TPβ W334Q and TPα Q333W substitutions conferred properties that corresponded to the other wild-type TP isoform. It has been shown that hydrophobic interactions are involved in the binding of CCT subunits to actin, VHL, and Gβ proteins (Kabir *et al.*, 2011). In particular, replacement of Trp^{117} substantially reduced the binding of the VHL protein to CCT (Feldman *et al.*, 2003), similar to what we observed for TPβ. It may be that CCT-complex proteins serve to facilitate early interactions between receptors and Gβ proteins during their biosynthesis and favor their proper assembly (Dupré *et al.*, 2006). However, the fact that we identified a single residue, Trp^{334}, that dictates the interaction between CCT7 and TPα or TPβ and their maturation and trafficking properties strongly supports that CCT7 acts, at least in part, directly on the receptors.

It might be counterintuitive that TPβ Trp^{334} is a major determinant of the TPβ-CCT7 interaction but its mutation does not reduce total TPβ protein expression and promotes maturation and cell-surface expression of the receptor. It has been shown that depletion of a single CCT subunit leads to the codepletion of the other CCT/TRiC complex subunits (Freund *et al.*, 2014). Thus expression knockdown of CCT7 could destabilize or deplete the CCT/TRiC complex, leading to receptor aggregation and degradation. Furthermore, it is common for substrates using the chaperonin complex to interact with multiple subunits through distinct determinants (Zhuravleva and Radford, 2014). It is reasonable to speculate that GPCRs using the CCT/TRiC complex will interact with multiple domains of many CCT subunits. This could explain, in part, why TPβ W334Q displays decreased CCT7 binding but is still able to mature and fold correctly, perhaps by interacting with other CCT domains or subunits through its ICL3, for example. The fact that TPβ W334Q showed improved maturation and cell-surface expression compared with wild-type TPβ suggests that the CCT7 interaction with Trp^{334} retains TPβ in the CCT/TRiC folding process during or before ER processing. In this regard, it is interesting to note that CCT7 displays holdase activity for substrates, in that it possesses the ability to bind folding intermediates of client proteins and to prevent aggregation without actively participating in the folding process itself (Powis *et al.*, 2013). CCT7 was reported to have a low affinity for ATP and to be unable to bind it at

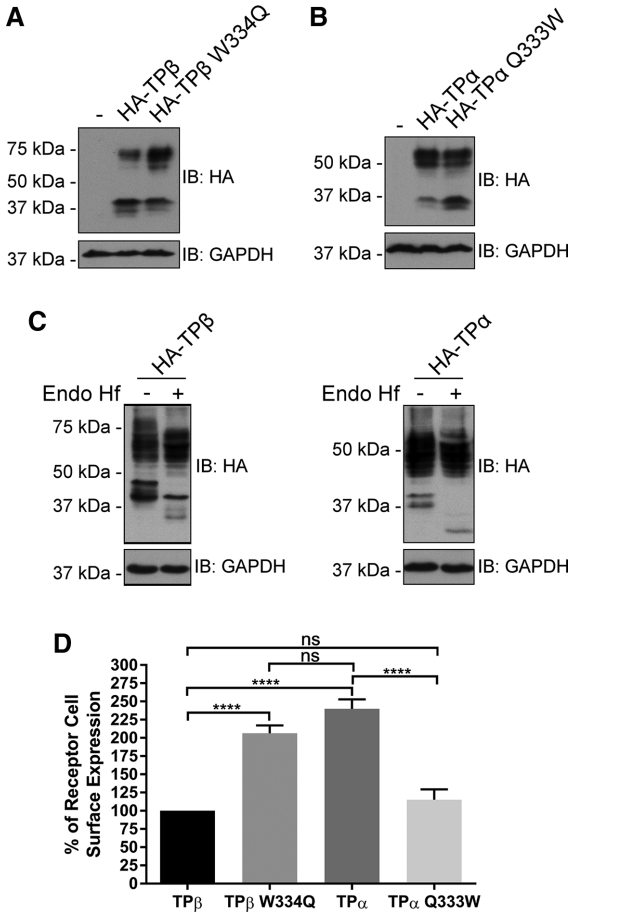

FIGURE 7: Trp^{334} is involved in TPβ maturation and cell-surface expression. (A) Lysates of HEK 293 cells transiently expressing HA-TPβ or HA-TPβ W334Q were analyzed by immunoblotting with HA-specific HRP-conjugated and GAPDH antibodies. (B) Lysates of HEK 293 cells transiently expressing HA-TPα or HA-TPα Q333W were analyzed by immunoblotting with HA-specific HRP-conjugated and GAPDH-specific antibodies. (C) Lysates from HEK 293 cells transiently expressing HA-TPβ or HA-TPα were subject to deglycosylation with Endo Hf as described in *Materials and Methods*. Immunoblotting was performed using HA-specific HRP-conjugated and GAPDH-specific antibodies. The blots shown are representative of three separate experiments. IB, immunoblotting. (D) Cell-surface receptor expression was measured in HEK 293 cells transiently expressing HA-TPβ, HA-TPβ W334Q, HA-TPα, or HA-TPα Q333W by ELISA using a monoclonal HA-specific antibody as described in *Materials and Methods*. The results are shown as the percentage of cell-surface receptor expression compared with HA-TPβ (TPβ, 100%). Results represent mean ± SEM of at least four independent experiments.

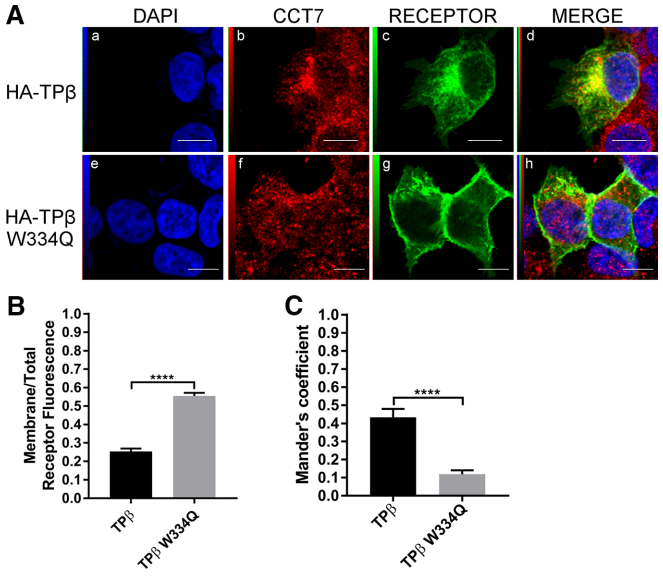

FIGURE 8: Characterization of the TPβ Trp^{334} mutant. (A) Confocal microscopy was performed on HEK 293 cells transiently expressing HA-TPβ (a–d) or TPβ W334Q (e–h). Cells were fixed, permeabilized, and labeled with goat anti-CCT7 IgG and mouse anti-HA IgG antibodies. Secondary antibodies used were Alexa Fluor 488–conjugated anti-mouse IgG and Texas red–conjugated anti-goat IgG. Cells were then stained with DAPI to visualize nuclei (a and e). The fourth panel on the right represents a merged image of the blue, green and red signals where the areas with high degree of colocalization between green-labeled receptors (c and g) and red-labeled CCT7 (b and f) appear yellow (d and h). Images shown are single confocal slices representative of at least four independent experiments and more than 100 observed cells. Scale bars: 10 μm. (B) Quantification of the membrane on total receptor fluorescence ratio was calculated using ImageJ software and was performed on at least 100 cells per condition. (C) Mander's colocalization coefficients represent the ratio of the green signal of the receptors overlapping the red signal of the aggresome and were calculated from at least 100 cells per condition. Results are presented as mean ± SEM.

physiological concentrations. High- and low-affinity CCT subunits were shown to be spatially segregated within two contiguous hemispheres in the CCT/TRiC ring, generating an asymmetric power stroke proposed to drive the folding cycle. This uncommon mode of ATP usage is thought to serve in coordinating a directional mechanism underlying the unique ability of CCT/TRiC to fold complex proteins (Reissmann *et al.*, 2012). Further experiments will be needed to fully understand the specificity and the role of the various CCT subunits and their binding determinants involved in GPCR folding.

In summary, we have characterized a direct and functional interaction between a subunit of the CCT/TRiC chaperonin complex and GPCRs. We have provided evidence that distinct nascent GPCRs can undergo alternative folding pathways and that CCT/TRiC is critical in preventing aggregation of some GPCRs and in promoting their proper maturation and expression.

MATERIALS AND METHODS

Reagents

Monoclonal anti-HA (3F10) antibody was from Roche Applied Science (Pleasanton, CA). Anti-GAPDH polyclonal antibody, anti–TCP-1$_\eta$ (CCT7) (E-20) goat polyclonal antibody, anti-β_2AR (H-73) polyclonal antibody, and protein G–agarose beads were purchased from Santa Cruz Biotechnology (Santa Cruz, CA). Texas Red anti-goat immunoglobulin G (IgG) was from Jackson ImmunoResearch (West Grove, PA). Alexa Fluor 488, Alexa Fluor 633 anti-rabbit IgG, and ProLong Gold antifade reagent were purchased from Invitrogen (Carlsbad, CA). Anti–c-Myc (9E10) monoclonal antibody was from Covance (Montreal, Canada). Anti–Myc-horseradish (HRP) polyclonal antibody was from Abcam (Toronto, Canada). Anti–rabbit-HRP IgG and anti–mouse-HRP IgG were purchased from GE Healthcare (Baie d'Urfé, Canada). Anti–goat-HRP IgG was from R&D Systems (Minneapolis, MN). Polyclonal anti-FLAG, the alkaline phosphatase–conjugated anti-mouse antibodies, and the alkaline phosphatase substrate kit were purchased from Sigma-Aldrich (Oakville, Canada). PROTEOSTAT Aggresome Detection Kit was

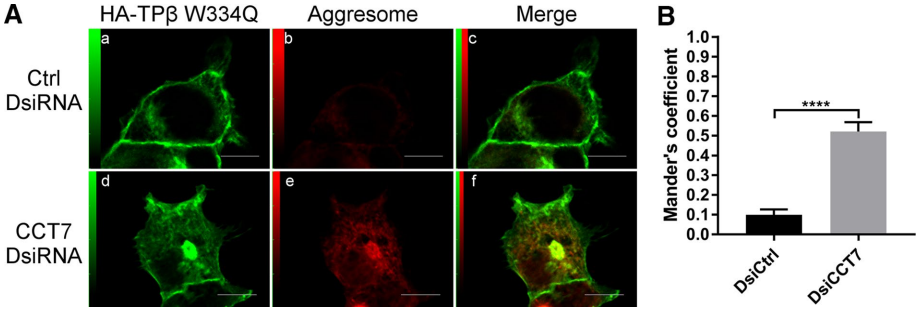

FIGURE 9: Targeting of the TPβ Trp^{334} mutant to the aggresome is diminished compared with wild-type TPβ in CCT7-depleted cells. (A) HEK 293 cells transiently expressing HA-TPβ W334Q were treated with control or CCT7 DsiRNAs. The cells were fixed, permeabilized, labeled with mouse anti-HA IgG, and stained with PROTEOSTAT aggresome dye. Alexa Fluor 633–conjugated anti-mouse IgG was used as the secondary antibody. The third images represent a merged image (c and f) of the green and red signals where the areas with high degree of colocalization between the green signal of the receptors (a and d) and red signal of the aggresome (b and e) appear yellow. Scale bars: 10 μm. Images shown are single confocal slices representative of at least four independent experiments and more than 250 observed cells. (B) Mander's colocalization coefficients represent the ratio of the green signal of the receptor overlapping the red signal of aggresomes and were calculated from at least 100 cells per condition. Results are presented as mean ± SEM.

from Enzo Life Sciences (Farmingdale, NY). Goat anti–GST-HRP antibody was purchased from Bethyl Laboratories (Montgomery, TX). Purified mouse anti-GM130 was purchased from BD Transduction Laboratories (San Jose, CA).

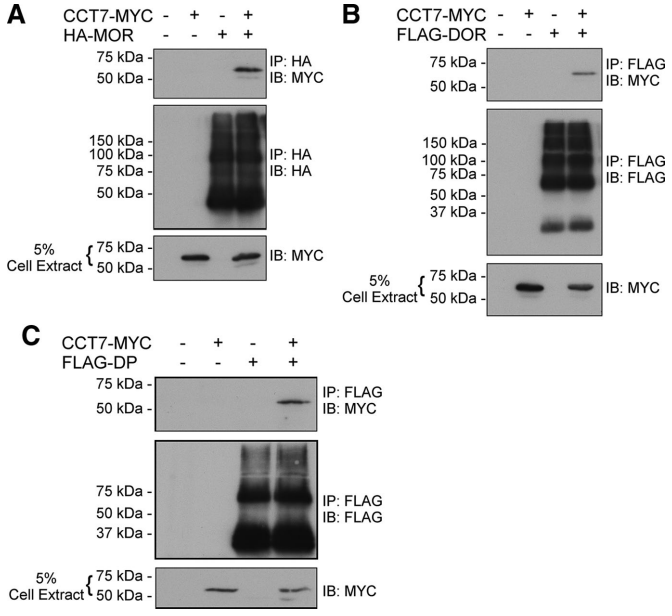

FIGURE 10: CCT7 coimmunoprecipitates with other GPCRs. (A) Lysates of HEK 293 cells transiently expressing HA-MOR (HA-tagged rat μ-opioid receptor) alone or with CCT7-MYC were immunoprecipitated with an HA-specific monoclonal antibody and analyzed by immunoblotting with MYC- and HA-specific HRP-conjugated antibodies. Lysates of HEK 293 cells transiently expressing FLAG-DOR (FLAG-tagged rat δ-opioid receptor; B) or FLAG-DP (FLAG-tagged prostaglandin D_2 receptor; C) alone or with CCT7-MYC were immunoprecipitated with a FLAG-specific monoclonal antibody and analyzed by immunoblotting with FLAG-specific polyclonal and HA-specific HRP-conjugated antibodies. The blots shown are representative of three separate experiments. IB, immunoblotting; IP, immunoprecipitation.

Plasmid constructs

CCT7 cDNA (NCBI accession NM_006429.3) was amplified from a human leukocyte cDNA library. MYC-tagged CCT7 construct was generated by PCR using the Phusion High-Fidelity PCR system (New England Biolabs, Whitby, Canada) and primers containing the MYC epitope in-frame with the N-terminus of the CCT7 open reading frame. The CCT7-MYC PCR fragment was digested with *Bam*HI and *Eco*RI and ligated into pcDNA3 and pRSET A vectors digested with the same restriction enzymes. Receptor constructs do not contain a signal peptide. HA-TPβ and HA-TPα site-directed mutagenesis was carried out by PCR using pcDNA3-HA-TPβ and pcDNA3-HA-TPα constructs (Parent *et al.*, 1999) as templates. TPβ pGEX-4T1 constructs were made as previously described (Cartier *et al.*, 2011). β_2AR and the yeast two-hybrid pAS2-1-TPβCT constructs were described previously (Parent *et al.*, 2009; Cartier *et al.*, 2011). The integrity of the coding sequences of all constructs was confirmed by dideoxy DNA sequencing. HA-MOR and FLAG-DOR constructs were a kind gift of Louis Gendron (Université de Sherbrooke).

Yeast two-hybrid screen

A yeast two-hybrid screen was performed following the two-hybrid system standard protocol (Gietz and Woods, 2002). Briefly, a plasmid containing the C-terminus of TPβ (pAS2-1-TPβCT) was transformed into the yeast strain pJ69-4α using the lithium yeast transformation protocol (Gietz and Woods, 2002). This stably transformed clone was then transformed with a human HeLa cell MATCHMAKER cDNA Library or with the empty pGAD-424 plasmid (Clontech, Mountain View, CA). Positive clones were initially selected for growth in the absence of histidine, and interactions were confirmed by growth on quadruple-selective medium (Trp^-, Leu^-, His^-, and Ade^-). pGADGH plasmids containing the library inserts from positive colonies were isolated and transformed into the DH10B bacterial strain. Plasmids were extracted from DH10B cells and transformed once more into yeast with either the bait (pAS2-1/TPβCT) or the negative control (pAS2-1) and plated on quadruple-selective medium (Trp^-, Leu^-, His^-, and Ade^-) to confirm the interaction. The selected plasmids were then sequenced by dideoxy DNA sequencing, and the identities of the clones were determined by using the NCBI BLAST alignment tool.

Cell culture and transfection

Human embryonic kidney 293 (HEK 293) cells were maintained in DMEM (Invitrogen) supplemented with 10% fetal bovine serum at 37°C in a humidified atmosphere containing 5% CO_2. Transient transfection of HEK 293 cells grown to 50–70% confluence was performed using the *Trans*IT-LT1 Reagent (Mirus, Madison, WI) according to the manufacturer's instructions. Empty pcDNA3 vector was added to keep the total DNA amount constant per plate. Stably TPβ- and β_2AR-expressing HEK 293 cells were generated as previously described (Azzi *et al.*, 2003; Parent *et al.*, 2008) and cultured the same way as transiently transfected cells except for the addition of 200 μg/ml of G418.

The synthetic duplex oligonucleotide named HSC.RNAI. N006429.12.4 targeting the human CCT7 gene and the negative control DsiRNA (DS NC1, catalogue number- 51-01-14-03) were

purchased from Integrated DNA Technologies (Coralville, IA). HEK 293 cells were transfected with 50 nM oligonucleotides using the Lipofectamine 2000 transfection reagent (Invitrogen) according to the manufacturer's recommendations, except for the following modifications: Cells were seeded directly into the transfection mix at twice the cell density indicated in the basic protocol. Reverse transcriptase-PCRs were carried out to confirm that the CCT7 DsiRNAs did not reduce the mRNA levels of the receptors.

Immunoprecipitations

HEK 293 cells were transiently transfected with the indicated constructs and maintained as described above for 48 h. Cells were then washed with ice-cold phosphate-buffered saline (PBS) and harvested in 300 µl of lysis buffer (150 mM NaCl, 50 mM Tris, pH 8.0, 0.5% deoxycholate, 0.1% SDS, 10 mM $Na_4P_2O_7$, 1% IGEPAL, and 5 mM ethylenediaminetetraacetic acid) supplemented with protease inhibitors (10 µM pepstatin, 10 µM antipain, 10 µM leupeptin, and 10 µM chymostatin [Sigma-Aldrich]). After 60 min of incubation in lysis buffer at 4°C with rotation, the lysates were then centrifuged for 20 min at 14,000 × *g* at 4°C. One microgram of specific antibodies was added to the supernatant. After 3 h of incubation at 4°C with rotation, 40 µl of 50% protein G–agarose beads was added, followed by overnight incubation at 4°C. Samples were then centrifuged for 1 min in a microcentrifuge and washed four times with 1 ml of lysis buffer. Immunoprecipitated proteins were eluted by addition of 35 µl of SDS sample buffer, followed by a 60 min incubation at room temperature. Initial lysates and immunoprecipitated proteins were analyzed by SDS–PAGE and immunoblotting with specific antibodies. Endogenous immunoprecipitations were performed in native HEK 293 cells. Cells were harvested and processed as described above, except proteins were immunoprecipitated overnight using 2 µg TCP-1_n (CCT7)-specific or appropriate control antibodies and 40 µl of 50% protein G–agarose beads.

Immunofluorescence staining and confocal microscopy

For colocalization experiments, HEK 293 cells stably expressing HA-β_2AR or HA-TPβ were plated in six-well plates at a density of 5×10^4 cells/well directly onto coverslips coated with 0.1 mg/ml poly-L-lysine (Sigma-Aldrich) and transfected with control or CCT7-specific DsiRNAs. The cells were fixed after a 72 h incubation with 2% (vol/vol) paraformaldehyde in PBS for 30 min at 4°C. Subsequently cells were washed twice with PBS and permeabilized for 10 min with 0.1% Triton X-100 in PBS and blocked for 30 min with 0.1% Triton X-100 in PBS containing 0.5% (wt/vol) bovine serum albumin (BSA) at room temperature. After two washing steps with 0.1% Triton X-100 in PBS, cells were incubated 2 h with HA-specific and CCT7-specific (not for IgG Ctrl conditions) antibodies diluted in blocking buffer at room temperature. The cells were washed twice with permeabilization buffer, blocked again for 10 min, and incubated with appropriate secondary antibodies for 60 min at room temperature or with the Proteostat aggresome dye according to the manufacturer's recommendations. Cells were then washed three times with PBS, and coverslips were mounted using ProLong Gold antifade reagent. Confocal microscopy was performed using a scanning confocal microscope (FV1000; Olympus, Richmond Hill, Canada) coupled to an inverted microscope with a 60× oil-immersion objective (Olympus), and all laser parameters were conserved between all image acquisitions for the same figure. Images were processed using Fluoviewer 2.0 software (Olympus), and Mander's colocalization coefficients (Dunn *et al.*, 2011) were calculated using the same threshold for fluorescent background elimination across all images, since they were acquired with the same parameters.

Measurement of cell-surface receptor expression by ELISA

Quantification of cell-surface receptor expression was carried out as we described before (Binda *et al.*, 2014). Briefly, 5×10^4 HEK 293 cells stably expressing HA-β_2AR or HA-TPβ were plated in 24-well plates precoated with 0.1 mg/ml poly-L-lysine (Sigma-Aldrich). Cells were transfected with the indicated DsiRNAs and then maintained for an additional 72 h. The cells were fixed in 3.7% (vol/vol) formaldehyde/Tris-buffered saline (TBS; 20 mM Tris-HCl, pH 7.5, and 150 mM NaCl) for 5 min at room temperature. Cells were then washed twice with TBS, and nonspecific binding was blocked by incubation with TBS containing 1% BSA for 30 min. A monoclonal HA-specific antibody was then added at a dilution of 1:2000 in TBS–BSA (1%) for 60 min. Following incubation with the primary antibody, cells were washed twice and blocked again with TBS–BSA (1%) for 10 min. Cells were then incubated with an alkaline phosphatase–conjugated goat anti-mouse antibody at 1:10,000 dilution in TBS–BSA (1%) for 60 min. Cells were washed twice with TBS, and 250 µl of a colorimetric alkaline phosphatase substrate was added as per the manufacturer's instructions. The plates were then incubated at 37°C until a yellow color appeared. The reaction was stopped by the addition of 250 µl of NaOH (0.4 M). A 200 µl aliquot of the colorimetric reaction was taken, and the absorbance was measured at 405 nm using a Titertek Multiskan MCC/340 spectrophotometer. All conditions were done in triplicate for each experiment.

Recombinant protein production and histidine pull-down analysis

For production of His-tagged proteins, a PCR fragment corresponding to the cDNA coding for full-length CCT7 was inserted into the pRSETA expression vector (Invitrogen) as described above. This construct was used to produce the fusion protein in OverExpressTM C41 (DE3) *Escherichia coli* strain (Avidis, Roubais, France) by following the manufacturer's instructions. The recombinant proteins were purified using nickel–nitrilotriacetic acid–agarose resin (Qiagen, Toronto, Canada) as indicated by the manufacturer. The cDNA fragments coding for the C-terminus and intracellular loops of β_2AR or TPβ introduced in the pGEXT-4T1 vector (Amersham Biosciences, Baie d'Urfé, Canada) were used to produce GST fusion proteins in the OverExpressTM C41 (DE3) *E. coli* strain, which were purified using glutathione–Sepharose 4B beads (Amersham Biosciences) and eluted according to the manufacturer's indications. Purified recombinant proteins were analyzed by SDS–PAGE followed by Coomassie brilliant blue R-250 staining. Five micrograms of each GST-tagged fusion protein was incubated with 5 µg of the purified nickel–nitrilotriacetic acid–agarose His-tagged CCT7 in wash buffer (300 mM NaCl, 50 mM NaH_2PO_4, 20 mM imidazole, 0.5% Triton X-100, and 2 mM dithiothreitol) supplemented with protease inhibitors (9 nM pepstatin, 9 nM antipain, 10 nM leupeptin, and 10 nM chymostatin). Binding reactions were then washed three times with wash buffer. SDS sample buffer was added to the binding reactions, and the tubes were boiled for 5 min. The pull-down reactions were analyzed by Western blotting with the indicated specific antibodies.

Deglycosylation assays

Receptors were transiently expressed in HEK 293 cells in 60 mm plates, and cell lysates were prepared as described above. Protein concentration of samples was determined with the *DC* (detergent-compatible) Bio-Rad (St-Laurent, Canada) protein assay. For Endo Hf experiments, volumes of lysates corresponding to 40 µg protein were denatured in glycoprotein denaturing buffer 1×

(New England Biolabs) for 30 min at 37°C followed by the addition of glycobuffer 1× (New England Biolabs) and 10,000 U/ml of Endo Hf (New England Biolabs). Samples were incubated with the enzyme for 5 h at 37°C and analyzed by Western blot.

Statistical analysis

Statistical analysis was performed using Prism version 5.0 (GraphPad Software) using a two-tailed Student's *t* test or one-way analysis of variance with multiple comparisons. Data were considered significant when p values were < 0.05 (*), < 0.01(**), < 0.001 (***), or < 0.0001 (****). Nonsignificant values are abbreviated as "ns."

ACKNOWLEDGMENTS

This work was supported by a grant from the Natural Sciences and Engineering Research Council of Canada (to J.-L.P.) and the Canadian Institutes of Health Research (to T.E.H.). J.-L.P. is the holder of the André-Lussier Research Chair. S.G. and J.D. were recipients of scholarships from the Fonds de Recherche Québec-Santé.

REFERENCES

Achour L, Labbé-Jullié C, Scott MGH, Marullo S (2008). An escort for GPCRs: implications for regulation of receptor density at the cell surface. Trends Pharmacol Sci 29, 528–535.

Amit M, Weisberg SJ, Nadler-Holly M, McCormack EA, Feldmesser E, Kaganovich D, Willison KR, Horovitz A (2010). Equivalent mutations in the eight subunits of the chaperonin CCT produce dramatically different cellular and gene expression phenotypes. J Mol Biol 401, 532–543.

Audigier Y, Friedlandert M, Blobel G (1987). Multiple topogenic sequences in bovine opsin. Proc Natl Acad Sci USA 84, 5783–5787.

Azzi M, Charest PG, Angers S, Rousseau G, Kohout T, Bouvier M, Piñeyro G (2003). Beta-arrestin-mediated activation of MAPK by inverse agonists reveals distinct active conformations for G protein-coupled receptors. Proc Natl Acad Sci USA 100, 11406–11411.

Bakthavatsalam D, Soung RH, Tweardy DJ, Chiu W, Dixon RAF, Woodside DG (2014). Chaperonin-containing TCP-1 complex directly binds to the cytoplasmic domain of the LOX-1 receptor. FEBS Lett 588, 2133–2140.

Ball SK, Field MC, Tippins JR (2010). Regulation of thromboxane receptor signaling at multiple levels by oxidative stress-induced stabilization, relocation and enhanced responsiveness. PLoS One 5, 1–13.

Belmonte SL, Blaxall BC (2011). G protein coupled receptor kinases as therapeutic targets in cardiovascular disease. Circ Res 109, 309–319.

Bergmayr C, Thurner P, Keuerleber S, Kudlacek O, Nanoff C, Freissmuth M, Gruber CW (2013). Recruitment of a cytoplasmic chaperone relay by the A2A adenosine receptor. J Biol Chem 288, 28831–28844.

Berndt U, Oellerer S, Zhang Y, Johnson AE, Rospert S (2009). A signal-anchor sequence stimulates signal recognition particle binding to ribosomes from inside the exit tunnel. Proc Natl Acad Sci USA 106, 1398–1403.

Binda C, Génier S, Cartier A, Larrivée JF, Stankova J, Young JC, Parent JL (2014). A G protein-coupled receptor and the intracellular synthase of its agonist functionally cooperate. J Cell Biol 204, 377–393.

Cartier A, Parent A, Labrecque P, Laroche G, Parent J-L (2011). WDR36 acts as a scaffold protein tethering a G-protein-coupled receptor, G q and phospholipase C in a signalling complex. J Cell Sci 124, 3292–3304.

Conn PM, Ulloa-Aguirre A (2011). Pharmacological chaperones for misfolded gonadotropin-releasing hormone receptors. Adv Pharmacol 62, 109–141.

Cuéllar J, Martín-Benito J, Scheres SHW, Sousa R, Moro F, López-Viñas E, Gómez-Puertas P, Muga A, Carrascosa JL, Valpuesta JM (2008). The structure of CCT-Hsc70 NBD suggests a mechanism for Hsp70 delivery of substrates to the chaperonin. Nat Struct Mol Biol 15, 858–864.

Dekker C, Stirling PC, McCormack EA, Filmore H, Paul A, Brost RL, Costanzo M, Boone C, Leroux MR, Willison KR (2008). The interaction network of the chaperonin CCT. EMBO J 27, 1827–1839.

Deshaies RJ, Koch BD, Werner-Washburne M, Craig EA, Schekman R (1988). A subfamily of stress proteins facilitates translocation of secretory and mitochondrial precursor polypeptides. Nature 332, 800–805.

Dunn KW, Kamocka MM, Mcdonald JH (2011). A practical guide to evaluating colocalization in biological microscopy. J Physiol Cell Physiol 300, 723–742.

Dupré DJ, Hébert TE (2006). Biosynthesis and trafficking of seven transmembrane receptor signalling complexes. Cell Signal 18, 1549–1559.

Dupré DJ, Robitaille M, Éthier N, Villeneuve LR, Mamarbachi AM, Hébert TE (2006). Seven transmembrane receptor core signaling complexes are assembled prior to plasma membrane trafficking. J Biol Chem 281, 34561–34573.

Feldman DE, Spiess C, Howard DE, Frydman J, Drive C (2003). Tumorigenic mutations in VHL disrupt folding in vivo by interfering with chaperonin binding. Mol Cell 12, 1213–1224.

Filipeanu CM, de Vries R, Danser AHJ, Kapusta DR (2011). Modulation of α2C adrenergic receptor temperature-sensitive trafficking by HSP90. Biochim Biophys Acta Mol Cell Res 1813, 346–357.

Freund A, Zhong FL, Venteicher AS, Meng Z, Veenstra TD, Frydman J (2014). Proteostatic Control of telomerase function through TRiC-mediated folding of TCAB1. Cell 159, 1389–1403.

García-Mata R, Bebök Z, Sorscher EJ, Sztul ES, Cell PJTJ, To B (1999). Characterization and dynamics of aggresome formation by a cytosolic GFP-chimera. 146, 1239–1254.

Garcia-Mata R, Gao Y-S, Sztul E (2002). Hassles with taking out the garbage: aggravating aggresomes. Traffic 3, 388–396.

Gietz RD, Woods RA (2002). Transformation of yeast by lithium acetate/single-stranded carrier DNA/polyethylene glycol method. Methods Enzymol 350, 87–96.

Jacoby E, Bouhelal R, Gerspacher M, Seuwen K (2006). The 7TM G-protein-coupled receptor target family. ChemMedChem 1, 760–782.

Johnston JA, Ward CL, Kopito RR (1998). Aggresomes: a cellular response to misfolded proteins. J Cell Biol 143, 1883–1898.

Kabir MA, Uddin W, Narayanan A, Reddy PK, Jairajpuri MA, Sherman F, Ahmad Z (2011). Functional subunits of eukaryotic chaperonin CCT/TRiC in protein folding. J Amino Acids 2011, 843206.

Kasembeli M, Lau WCY, Roh SH, Eckols TK, Frydman J, Chiu W, Tweardy DJ (2014). Modulation of STAT3 folding and function by TRiC/CCT chaperonin. PLoS Biol 12, e1001844.

Kirstein-Miles J, Scior A, Deuerling E, Morimoto RI (2013). The nascent polypeptide-associated complex is a key regulator of proteostasis. EMBO J 32, 1451–1468.

Knee KM, Sergeeva OA, King JA (2013). Human TRiC complex purified from HeLa cells contains all eight CCT subunits and is active in vitro. Cell Stress Chaperones 18, 137–144.

Lappano R, Maggiolini M (2012). GPCRs and cancer. Acta Pharmacol Sin 33, 351–362.

Laroche G, Lépine MC, Thériault C, Giguère P, Giguère V, Gallant MA, De Brum-Fernandes A, Parent JL (2005). Oligomerization of the α and β isoforms of the thromboxane A2 receptor: relevance to receptor signaling and endocytosis. Cell Signal 17, 1373–1383.

Llorca O, McCormack EA, Hynes G, Grantham J, Cordell J, Carrascosa JL, Willison KR, Fernandez JJ, Valpuesta JM (1999). Eukaryotic type II chaperonin CCT interacts with actin through specific subunits. Nature 402, 693–696.

McCallum CD, Do H, Johnson AE, Frydman J (2000). The interaction of the chaperonin tailless complex polypeptide 1 (TCP1) ring complex (TRiC) with ribosome-bound nascent chains examined using photo-cross-linking. J Cell Biol 149, 591–601.

Meimaridou E, Gooljar SB, Ramnarace N, Anthonypillai L, Clark AJL, Chapple JP (2011). The cytosolic chaperone hsc70 promotes traffic to the cell surface of intracellular retained melanocortin-4 receptor mutants. Mol Endocrinol 25, 1650–1660.

Melville MW, Mcclellan AJ, Meyer AS, Frydman J, Darveau A (2003). The Hsp70 and TRiC/CCT chaperone systems cooperate in vivo to assemble the von Hippel-Lindau tumor suppressor complex. Mol Cell Biol 23, 3141–3151.

Ngosuwan J, Wang NM, Fung KL, Chirico WJ (2003). Roles of cytosolic Hsp70 and Hsp40 molecular chaperones in post-translational translocation of presecretory proteins into the endoplasmic reticulum. J Biol Chem 278, 7034–7042.

Parent A, Hamelin E, Germain P, Parent J-L (2009). Rab11 regulates the recycling of the beta2-adrenergic receptor through a direct interaction. Biochem J 418, 163–172.

Parent A, Laroche G, Hamelin E, Parent J-L (2008). RACK1 regulates the cell surface expression of the G protein-coupled receptor for thromboxane A(2). Traffic 9, 394–407.

Parent J, Labrecque P, Orsini MJ, Benovic JL (1999). Internalization of the TXA 2 receptor α and β isoforms. J Biol Chem 274, 8941–8948.

Pause B, Diestelkötter P, Heid H, Just WW (1997). Cytosolic factors mediate protein insertion into the peroxisomal membrane. FEBS Lett 414, 95–98.
Plath K, Rapoport TA (2000). Spontaneous release of cytosolic proteins from posttranslational substrates before their transport into the endoplasmic reticulum. J Cell Biol 151, 167–178.
Plimpton RL, Cuéllar J, Lai CWJ, Aoba T, Makaju A, Franklin S, Mathis AD, Prince JT, Carrascosa JL, Valpuesta JM, Willardson BM (2015). Structures of the Gβ-CCT and PhLP1–Gβ-CCT complexes reveal a mechanism for G-protein β-subunit folding and Gβγ dimer assembly. Proc Natl Acad Sci USA 112, 2413–2418.
Powis K, Schrul B, Tienson H, Gostimskaya I, Breker M, High S, Schuldiner M, Jakob U, Schwappach B (2013). Get3 is a holdase chaperone and moves to deposition sites for aggregated proteins when membrane targeting is blocked. J Cell Sci 126, 473–483.
Raychowdhury MK, Yukawa M, Collins LJ, McGrail SH, Craig Kent K, Ware JA (1994). Alternative splicing produces a divergent cytoplasmic tail in the human endothelial thromboxane A2 receptor. J Biol Chem 269, 19256–19261.
Reissmann S, Joachimiak LA, Chen B, Meyer AS, Nguyen A, Frydman J (2012). A gradient of ATP affinities generates an asymmetric power stroke driving the chaperonin TRIC/CCT folding cycle. Cell Rep 2, 866–877.
Roux BT, Cottrell GS (2014). G protein-coupled receptors: what a difference a "partner" makes. Int J Mol Sci 15, 1112–1142.
Roy SJ, Glazkova I, Fréchette L, Iorio-Morin C, Binda C, Pétrin D, Trieu P, Robitaille M, Angers S, Hébert TE, Parent JL (2013). Novel, gel-free proteomics approach identifies RNF5 and JAMP as modulators of GPCR stability. Mol Endocrinol 27, 1245–1266.
Salemi LM, Almawi AW, Lefebvre KJ, Schild-Poulter C (2014). Aggresome formation is regulated by RanBPM through an interaction with HDAC6. Biol Open 3, 418–430.
Saliba RS, Munro PMG, Luthert PJ, Cheetham ME (2002). The cellular fate of mutant rhodopsin: quality control, degradation and aggresome formation. J Cell Sci 115, 2907–2918.
Salon JA, Lodowski DT, Palczewski K (2011). The significance of G protein-coupled receptor. Pharmacol Rev 63, 901–937.
Schülein R, Westendorf C, Krause G, Rosenthal W (2012). Functional significance of cleavable signal peptides of G protein-coupled receptors. Eur J Cell Biol 91, 294–299.
Spiess C, Miller EJ, McClellan AJ, Frydman J (2006). Identification of the TRiC/CCT substrate binding sites uncovers the function of subunit diversity in eukaryotic chaperonins. Mol Cell 24, 25–37.
Tao YX, Conn PM (2014). Chaperoning G protein-coupled receptors: from cell biology to therapeutics. Endocr Rev 35, 602–647.
Thériault C, Rochdi MD, Parent JL (2004). Role of the Rab11-associated intracellular pool of receptors formed by constitutive endocytosis of the beta isoform of the thromboxane A2 receptor (TP beta). Biochemistry 43, 5600–5607.
Valpuesta JM, Martin-Benito J, Gomez-Puerta P, Carrascosa JL, Willison KR (2002). Structure and function of a protein folding machine: the eukaryotic chaperonin CCT. FEBS Lett 529, 11–16.
Vassart G, Costagliola S (2011). G protein-coupled receptors: mutations and endocrine diseases. Nat Rev Endocrinol 7, 362–372.
Watanabe Y, Tatebe H, Taguchi K, Endo Y, Tokuda T, Mizuno T, Nakagawa M, Tanaka M (2012). p62/SQSTM1-dependent autophagy of Lewy body-like α-synuclein inclusions. PLoS One 7, 1–12.
White DA, Buell AK, Knowles TPJ, Welland ME, Dobson CM (2010). Protein aggregation in crowded environments. Am Chem Soc 132, 5170–5175.
Wigley CW, Fabunmi RP, Lee MG, Marino CR, Muallem S, DeMartino GN, Thomas PJ (1999). Dynamic association of proteasomal machinery with the centrosome. J Cell Biol 145, 481–490.
Yam AY, Xia Y, Lin H-T J, Burlingame A, Gerstein M, Frydman J (2008). Defining the TRiC/CCT interactome links chaperonin function to stabilization of newly made proteins with complex topologies. Nat Struct Mol Biol 15, 1255–1262.
Young JC, Agashe VR, Siegers K, Hartl FU (2004). Pathways of chaperone-mediated protein folding in the cytosol. Nat Rev Mol Cell Biol 5, 781–791.
Zhuravleva A, Radford SE (2014). How TriC folds tricky proteins. Cell 159, 1251–1252.